NUMERICAL ANALYSIS OF HIGH PRESSURE COLD BEND PIPE TO INVESTIGATE THE BEHAVIOUR OF TENSION SIDE FRACTURE

Celal Cakiroglu, Amin Komeili, Samer Adeeb, Roger Cheng, Millan Sen

ABSTRACT

The cold bend pipelines may be affected by the geotechnical movements due to unstable slopes, soil type and seismic activities. An extensive experimental study was conducted by Sen et al. in 2006 to understand the buckling behaviour of cold bend pipes. In their experiments, it was noted that one high pressure X65 pipe specimen failed under axial and bending loads due to pipe body tensile side fracture which occurred after the development of a wrinkle. The behaviour of this cold bend pipe specimen under bending load has been investigated numerically to understand the conditions leading to pipe body tension side fracture following the compression side buckling. Bending load has been applied on a finite element model of the cold bend by increasing the curvature of it according to the experimental studies conducted by Sen [1]. The bending loads have been applied on the model with and without internal pressure. The distribution of the plastic strains and von Mises stresses as well as the load – displacement response of the pipe have been compared for both load cases. In this way the experimental results obtained by Sen [1] have been verified. The visualization of the finite element analysis results showed that pipe body failure at the tension side of the cold bend takes place under equal bending loads only in case of combined loading with internal pressure.

INTRODUCTION

Pipelines can be subjected to excessive tensile and bending forces due to a variation of geotechnical conditions like soil slope instability or soil liquefaction during an earthquake as well as due to significant temperature differences between the operating temperature of gas pipeline and the outer temperature. Cold bends are applied at locations where it is necessary to adjust the pipe orientation according to changing slope of the trench or to change the horizontal orientation of the pipe. The procedure of cold bending causes residual stresses in the pipe and changes the material properties by loading the extrados of the bend beyond the yield stress in tension and loading the intrados of the bend beyond the yield stress in compression. The applied forces caused by soil – pipe interaction induce deformations in the pipe which usually accumulate adjacent to cold bends. As a result increased curvature of the cold bend may cause buckling or fracture of the pipe.

In order to investigate the behaviour of cold bend pipes under axial load, in-plane bending and internal pressure, an extensive research project has been conducted by Sen, [1], [2], [3]. In the scope of this research project a total of 8 full scale specimens with different pipe geometries, material properties and internal pressures were tested. In one of these experiments the behaviour of an X65 cold bend pipe under in-plane bending load and internal pressure was tested. The experimental setup for a specimen under bending loads is demonstrated in Figure 2. The outcome of this experiment was that after the buckling load of the pipe was reached the further loading of the pipe eventually led to a sudden fracture on the tension side of the pipe and the loss of containment capability. Similar experiments have been carried out by Miki et al. [4] which showed the influence of internal pressure on ductile fracture behaviour using pressurized and un-pressurized tension tests in the presence of girth weld defects.

In this paper the behaviour of a cold bend pipe by a combination of internal pressure and bending load has been simulated for the case of a specimen which is demonstrated in Figure 1 that exhibited tension side fracture following compression side buckling in order to obtain a better understanding of this rare but

critical phenomenon. This is a type of pipe failure which is rarely considered during design, whereby tensile failure is generally only considered to be at risk at girth weld locations. Also this occurs rarely in the testing of pipes although the loading is realistic and immense energy release takes place during the fracture of a gas pipeline which leads to a sudden loss of the containment capability of the pipe. This energy release could have some harmful effects on the environment. Therefore it is crucial to investigate the allowable deformations of a cold bend under this load case further for a better understanding and prevention of the tension side fracture of cold bends. The main objective of this paper is to investigate the buckling at the location of cold bends and how it might eventually lead to the loss of containment capability of the pipe due to fracture in the tension side of the buckle. Furthermore this investigation is used to define a criterion for the allowable curvature and bending angle of a cold bend pipe in the field conditions to prevent the fracture and the loss of containment capability of the pipe.

Finite element analysis has been carried out for this purpose simulating the cold bend pipe under closing mode loading where the extrados of the bend is under tensile loading and the intrados of the bend is under compressive loading which is the most critical case because of the compressive residual stresses in the intrados of the bend. Displacement controlled loading has been applied increasing the curvature of the pipe incrementally beyond the onset of local buckling until fracture takes place at the extrados of the bend. In this way both the critical buckling strain and the post-buckling response of the pipe as well as the allowable deformations before pipe failure could be examined.

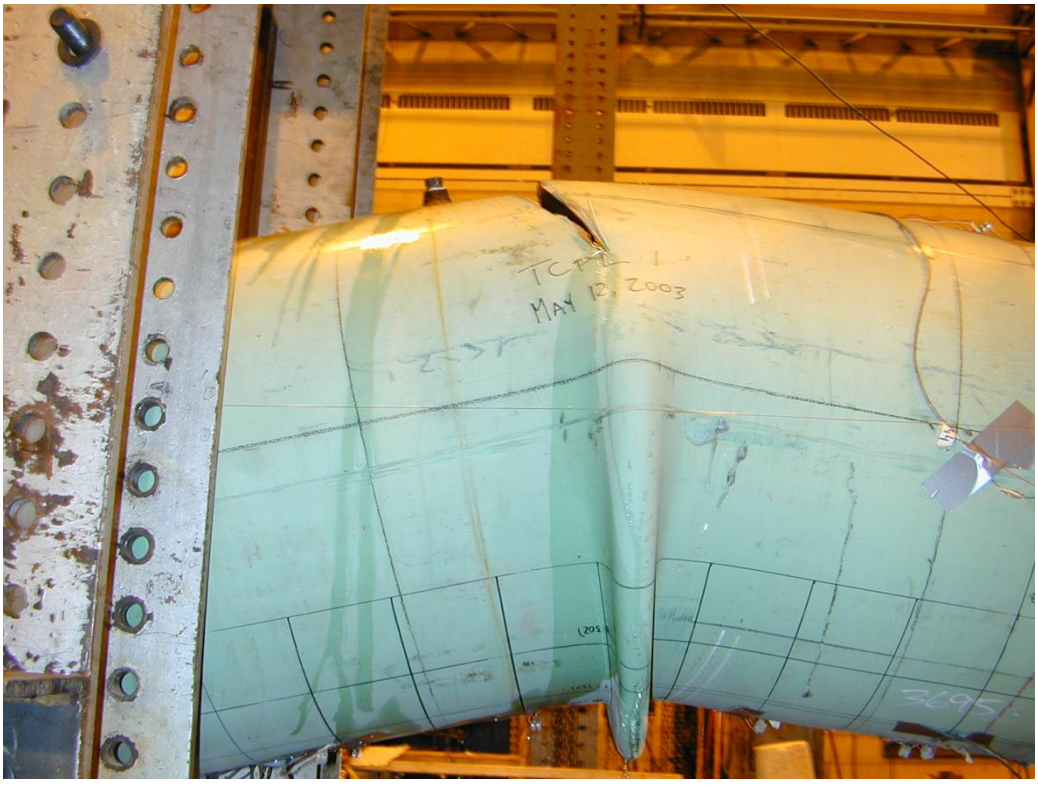

Figure 1: Wrinkle and Fracture of the Test Specimen [1]

NUMERICAL ANALYSIS OF THE EXPERIMENT

The behaviour of an X65 cold bend pipe by a combination of internal pressure and bending load has been analyzed numerically using the finite element analysis software ABAQUS Version 6.10. The experimental studies carried out by Sen [2] exhibiting a tension side fracture following the compression side buckling of a cold bend by a combination of bending load and internal pressure were simulated. The grade of the simulated pipe corresponds to 448 MPA specified minimum yield strength. In the finite element model the Young' s modulus of 210700 MPA has been used. To simulate the plastic behaviour of the material a metal plasticity model with isotropic hardening has been applied. In this model a linear increase in the stress from 448.16 MPA to 530.9 MPA is assumed for a plastic strain increase of 5%. During the pre-processing of the model geometry the symmetry of the cold bend has been used and one quarter of a full scale test specimen having an outer section diameter of 761.5 mm, diameter to wall thickness ratio of 93 and a nominal wall thickness of 8.2 mm has been modeled which resulted in a significant reduction of the total number of elements and computational time. The simplification of the finite element model is also justified since the buckling of the specimen in the experimental studies occurs perpendicular to the applied in-plane moment and the out-of-plane displacement of the test specimen is constrained in the experimental setup. In order to model the curvature of the pipe which has a total length of 7454 mm, a horizontal length of 7400 mm and a bend angle of 12° has been introduced in two simulations; with and without internal pressure. Since the wall thickness of the pipe was small in comparison to its diameter, S4R shell elements have been selected and by both simulations the models have been meshed with 5204 elements. For the modeling of the collar part in Figure 2 the shell element thickness has been increased to 16 mm in order to prevent the buckling of the pipe in the sections close to the end plates, which is an undesirable type of buckling since it is caused by the testing setup and would not occur under field conditions. In order to apply appropriate symmetry boundary conditions the translation degree of freedom in the x- direction and the rotation degrees of freedom around the y- and z- axes have been constrained at the x-symmetry edge of the pipe. For the modeling of the z- symmetry the translation degree of freedom in the z- direction and the rotation degrees of freedom around the x – and y – axes have been constrained for the nodes along the longitudinal edges of the pipe. The endplate in the test setup was bolted to a heavy I-section moment arm that functioned to significantly increase its bending stiffness. In the finite element model the endplate was modeled by creating a node at the center of the pipe section at the pipe end, and applying a rigid beam constraint to connect the adjacent nodes around the pipe wall to the center of the pipe section. The center point of the pipe section then was connected to the loading pin which was located 600mm below the center point of the pipe by another rigid beam constraint. This rigid beam correlates to the heavy I section moment arm. For the node representing the loading pin the translation degree of freedom in the z-direction and the rotation degrees of freedom around the x- and y- axes have been constrained and the same boundary conditions have been transmitted to the adjacent nodes on the pipe end by rigid body constraints. The displacement controlled loading has been applied by prescribing the translation of the node representing the loading pin in x – and y directions. For both simulations a total displacement of 298.99 mm in x direction and 24.58 mm in –y direction have been applied to the node which is connected to the edge of the pipe with rigid beam constraints. The application of the rigid beam constraints and the displacements is demonstrated in Figure 3. The eccentricity of the applied displacement in the x – direction created significant bending moment. By the simulation of the load case with internal pressure, 7.7 MPa internal pressure has been applied as the first load step, and the displacement has been applied as the second load step. The bending moment induced by the internal pressure acting on the endplate has been applied on the node representing the loading pin in the z-direction.

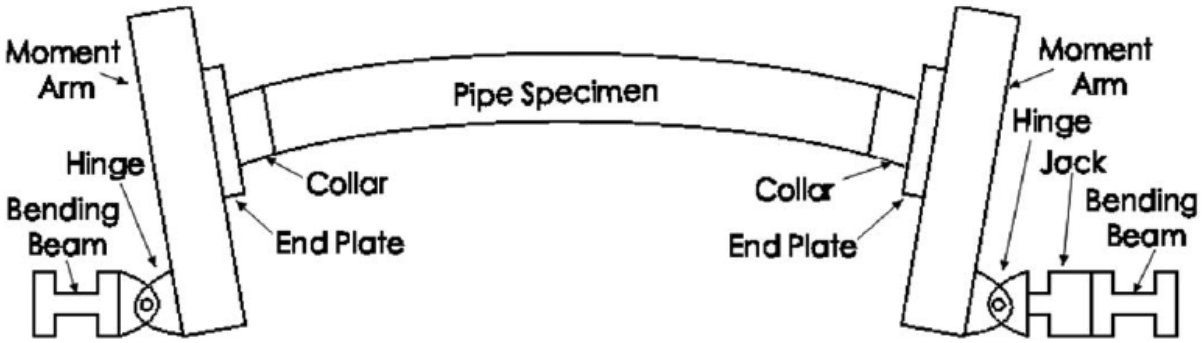

Figure 2: Schematic of the experimental setup [2]

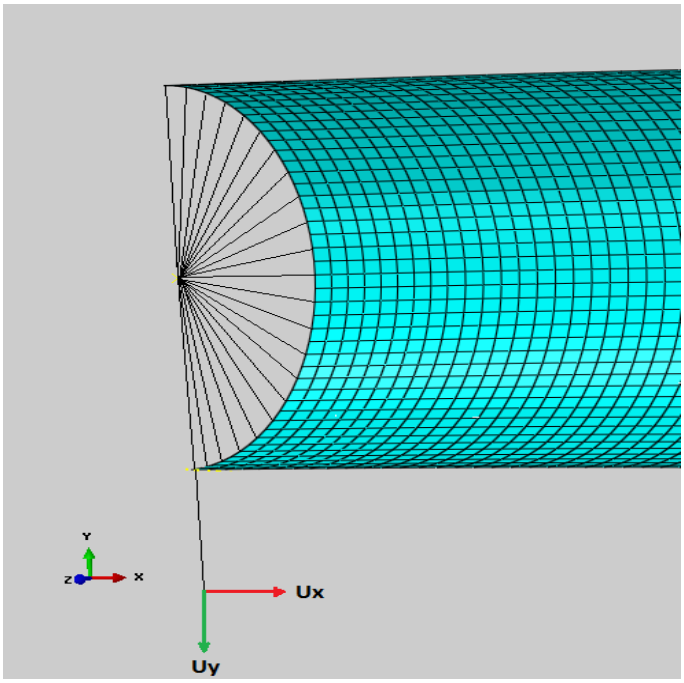

Figure 3: Applied displacements and rigid beam constraints

RESULTS

Figure 4 shows the distribution of the plastic strain in the post-buckling range after the displacement controlled loading has been completed. The initiation of buckling on the compression side of the pipe took place almost immediately after the start of the simulation as the load – displacement curve in Figure

6 demonstrates the decreasing stiffness of the pipe during the loading. It is clear from Figure 4 that throughout the post-buckling range no plastic strain can be observed on the tension side of the pipe whereas on the compression side the plastic strain is concentrated at the wrinkle location where the majority of the deformation associated with the loading took place. This observation indicates that the tension side fracture of the cold bend in the experimental studies is mainly caused by the internal pressure. In addition to the plastic strain also the distribution of the von Mises stresses have been visualized for loading without internal pressure in Figure 5. The visualization of the von Mises stress distribution also confirms that the stresses are concentrated at the compression side of the wrinkle location.

The plastic strain distribution in the case where displacement controlled loading has been applied on the pressurized pipe is demonstrated in Figure 7. It can be clearly observed that plastic strains have been concentrated on the tension side of the pipe at the wrinkle location where they eventually caused the failure of the pipe. The plastic strains started to develop at the compression side of the wrinkle location from the first load increment of the displacement controlled loading. After reaching a level of about 37%, no considerable increase of the plastic strain at the compression side has been observed during the entire simulation whereas the plastic strain at the tension side continued to increase until the failure on the tension side. Figure 8 shows the von Mises stress distribution for the case of combined loading with internal pressure. The magnitude of the stresses and the distorted element shapes on the tension side indicates the failure of the pipe on the tension side.

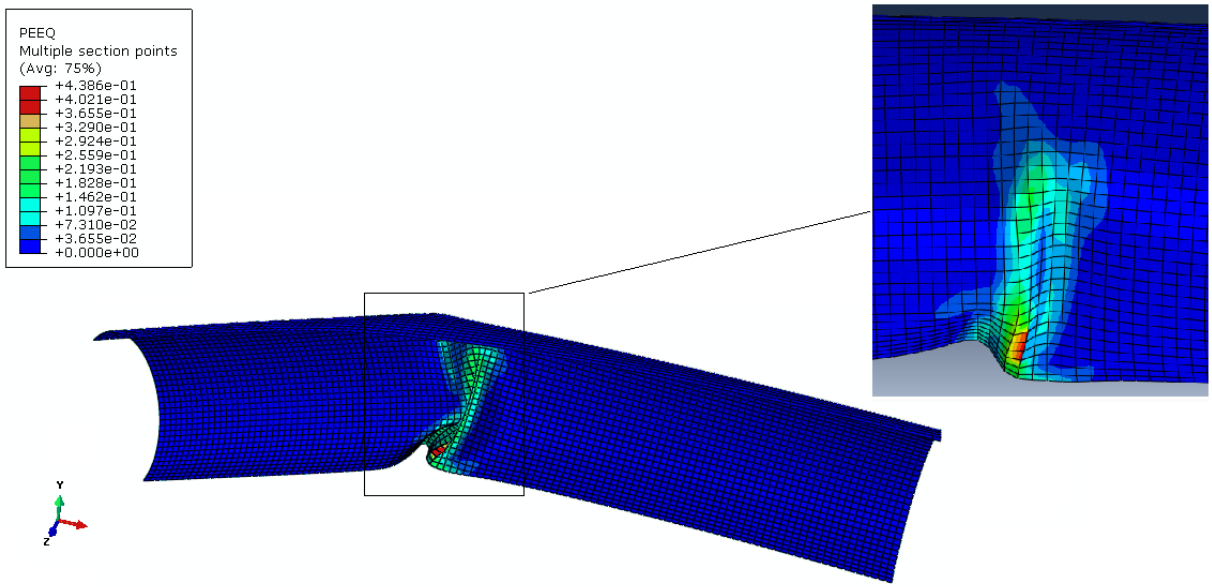

Figure 4: Plastic strain distribution under bending load without internal pressure

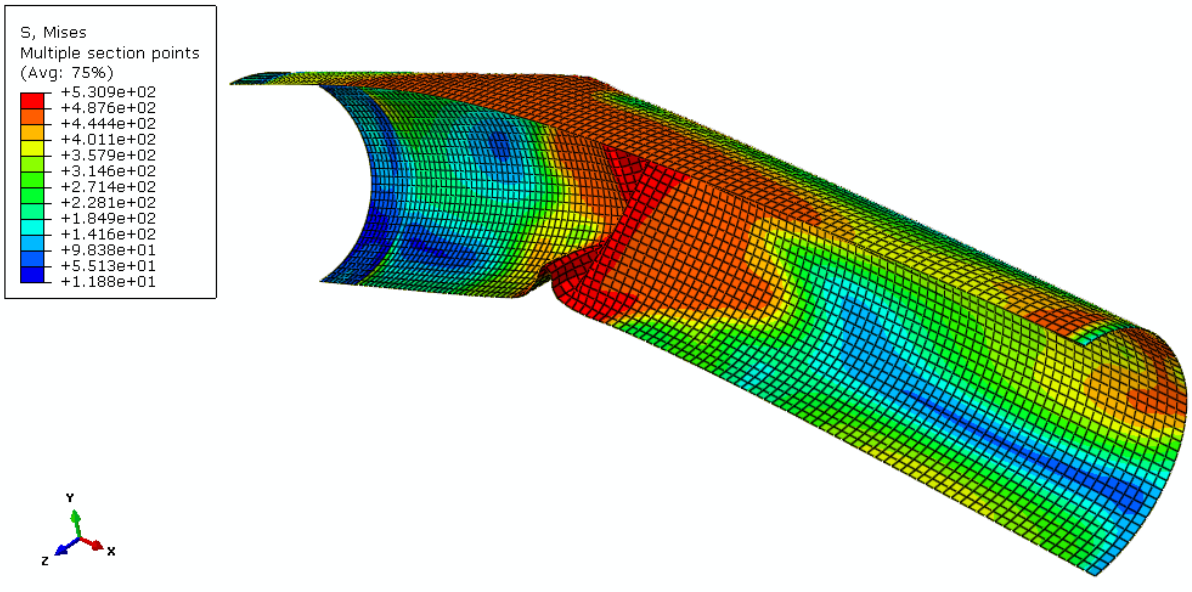

Figure 5: Von Mises stress distribution under bending load without internal pressure

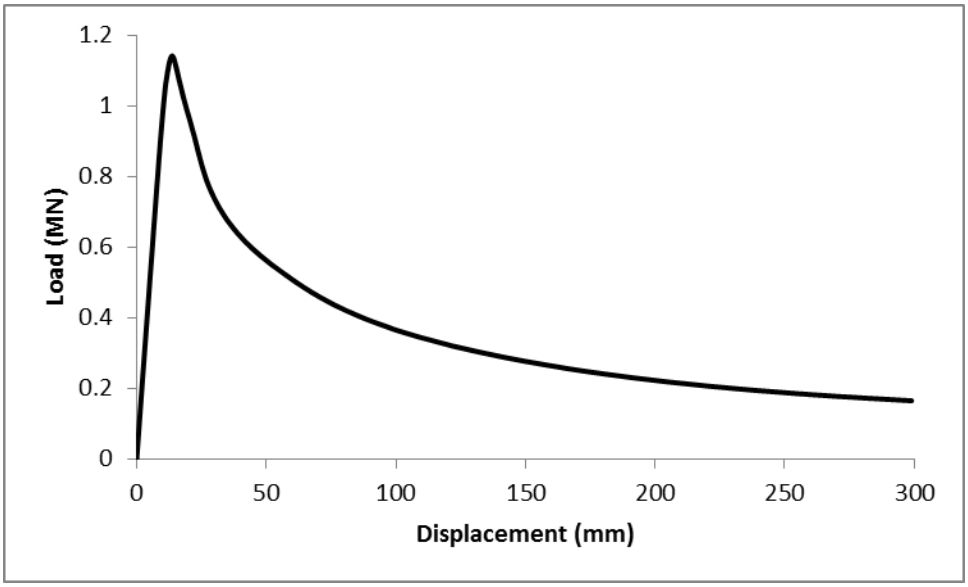

Figure 6: Load - displacement response under bending load without internal pressure

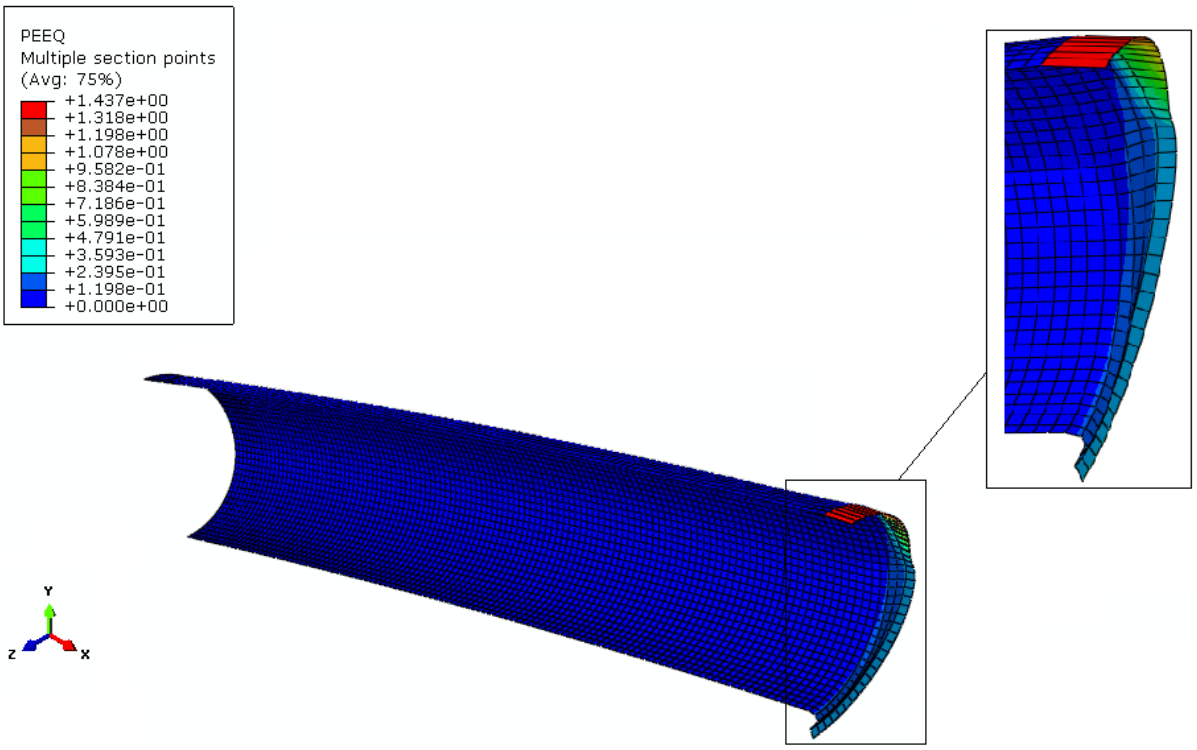

Figure 7: Plastic strain distribution under bending load and internal pressure

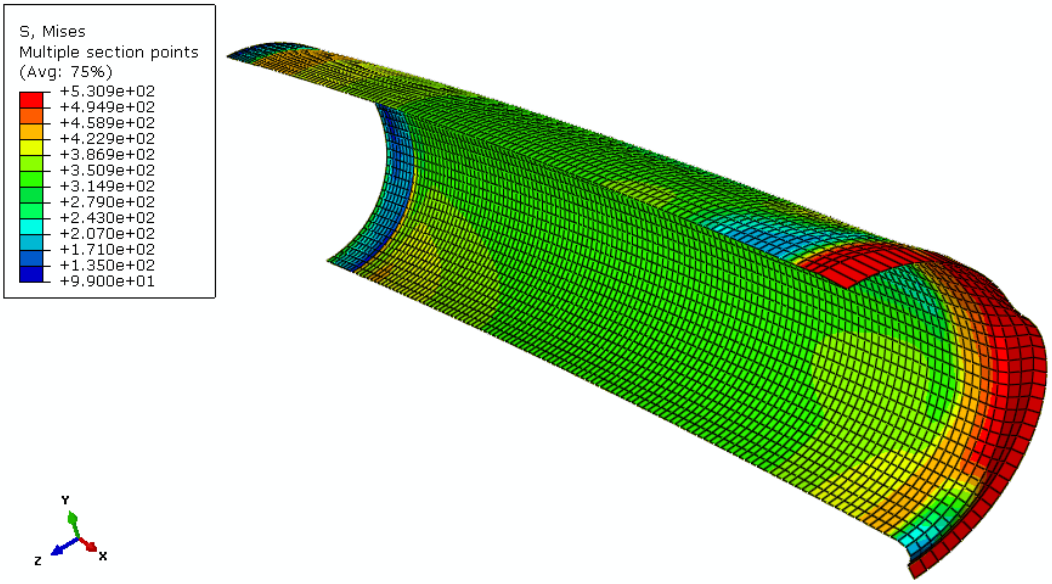

Figure 8: Von Mises stress distribution under bending load and internal pressure

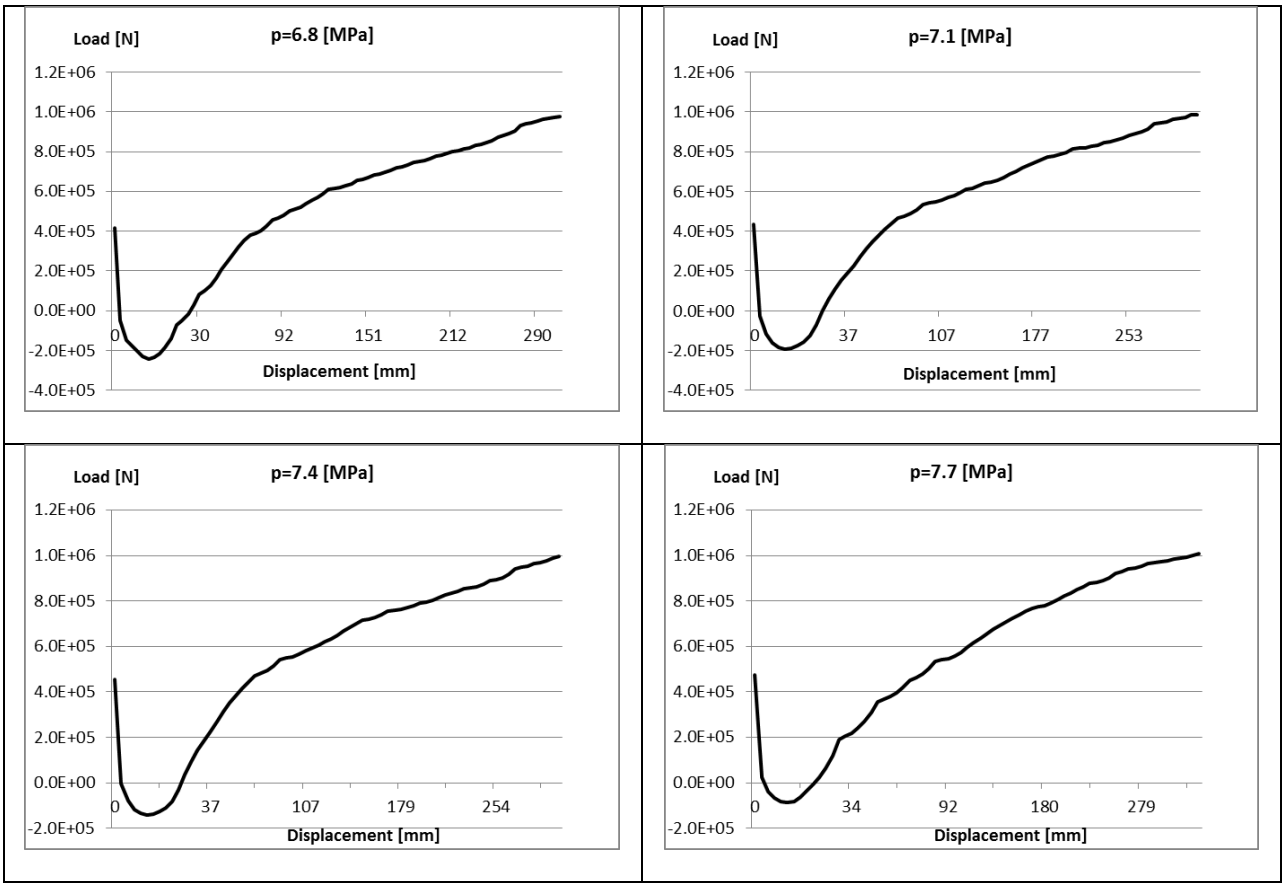

Figure 9: Load - displacement response under bending load and internal pressure

It can be observed that there are minor differences between the load – displacement curves for the different internal pressure cases. The common feature of the 4 graphs is that the buckling in the compression side of the pipe takes place in the early stages of the applied bending load although there is no sharp transition to the post-buckling. These curves have been generated by plotting the variation of the reaction force at the loading pin with respect to the displacement of the loading pin in the positive x-direction. Since the increase in the pipe curvature is proportional to the applied displacement and since the model maximum moment is proportional to the reaction force in the x-direction, these curves also give an idea about the change of the maximum moment in the system with respect to the cold bend curvature. The graphs in Figure 9 show that the sign of the reaction force changes directly after the start of the displacement load step. This change of sign is related to the direction of the applied forces due to the internal pressure and due to the external displacement loading. Since these two applied forces have opposite signs it follows that the greater forces caused by the internal pressure lead to negative values of the total reaction force at the beginning of the displacement load step. As the applied curvature increases the magnitude of the associated reaction forces exceeds the magnitude of the reaction forces associated with the internal pressure and the sign of the total reaction force becomes positive.

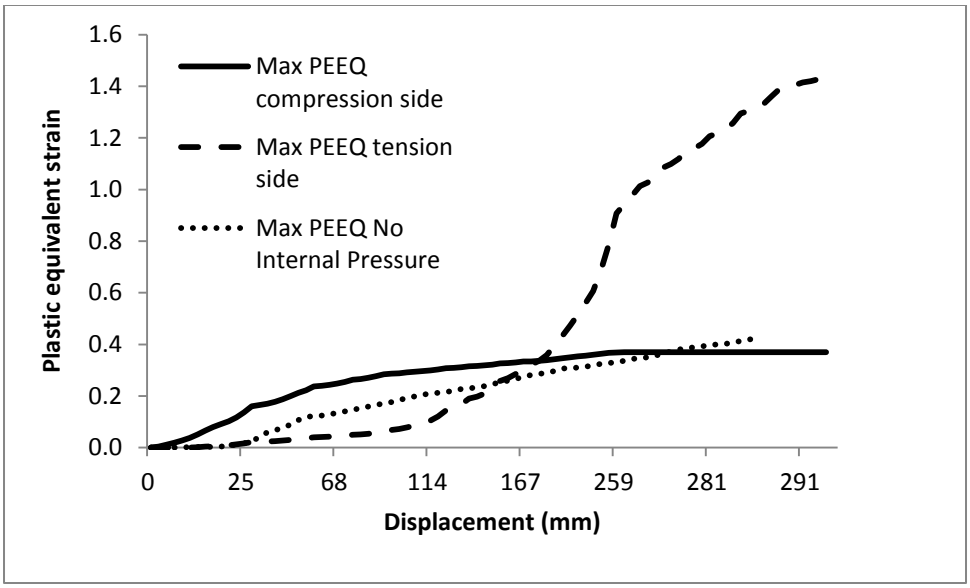

Figure 10: Comparison of maximum equivalent plastic strain curves

Figure 10 demonstrates a comparison of the maximum equivalent plastic strains at the compression and tension sides of the cold bend under bending load with internal pressure as well as the maximum equivalent plastic strain under bending load without internal pressure. Figure 10 shows that for the load case with internal pressure, after 74% of the displacement loading has been applied the plastic strain on the compression side stays constant throughout the remaining load increments whereas the plastic strain on the tension side continues to increase. However at this stage of the displacement controlled loading a decrease in the slope of the curve showing the maximum plastic strain at the tension side is observed. This gives us a means for determining the amount of displacement loading which shall not be exceeded in order not to risk the containment capability of the pipe. Using this method the allowable maximum bend angle and curvature of the cold bend can be calculated. Assuming that the axis of the cold bend pipe is contained within a circle of decreasing radius R during the entire simulation, the curvature κ of the cold bend can be approximated using the equation $\kappa = 1/R$. Calculating the cold bend radius when 74% of the displacement loading has been applied gives the criterion for the maximum allowable curvature. The investigation of the plastic strain in case of loading without internal pressure shows that the curve of maximum plastic strain variation for this case has a development similar to the curve for compression side maximum plastic strain in case of loading with internal pressure. In this case the maximum plastic strain continues to increase linearly in the last stages of the displacement loading.

DISCUSSION AND SUMMARY

Transportation of oil and natural gas from remote regions to the place of consumption requires the construction of pipelines crossing long distances. During this procedure it is necessary to change pipe orientation horizontally or vertically according to a variation of geotechnical conditions. In order to adjust the pipe orientation to the surrounding terrain, cold bends are frequently applied. However external forces

caused by longitudinal displacements along the pipeline due to a ground movement like an earthquake or bending loads applied on the pipe in case of a slope instability may lead to an accumulation of the strains in the locations of cold bends. Because of residual stresses and strains due to the cold bending procedure, cold bends are parts of a pipeline which are most prone to structural failure like instable buckling or fracture which makes it inevitable to study their behaviour under different types of loading experimentally and numerically.

In this paper numerical studies have been carried out in order to obtain a better understanding of the experimental results presented by Sen [1] about the tension side fracture and compression side buckling of a cold bend. This is a very critical type of pipe failure since immense energy release takes place during the fracture of a gas pipeline which leads to a sudden loss of the containment capability of the pipe and harmful effects on the environment. For this purpose the plastic strain and the von Mises stress distributions of the cold bend have been investigated under displacement controlled bending load with and without internal pressure. Visualization of the results for these two load cases indicated that internal pressure dramatically increases the von Mises stress and the plastic strain on the tension side of the cold bend at the location where wrinkling occurs which leads to the fracture of the pipe on the tension side eventually. On the other hand the plastic strain on the compression side stays almost constant throughout the simulation. A comparison of the response curves in Figure 6 and Figure 9 indicate that the presence of the internal pressure has a considerable effect on the load – deformation behaviour.

In case of loading with internal pressure the structural failure initiated as buckling and formation of wrinkles on the pipe intrados. The plastic strain reached its heighest level in the compression side and stayed constant in the post-buckling range. On the other hand the plastic strains in the pipe extrados continuously increased in the post-buckling range until the tensile side fracture occured. The change in the pipe geometry during this process is presented in Figure 11 where the y - coordinates of the nodes on a line separating the pipe in two equal parts in the longitudinal direction are plotted at the unloaded state, at the state when the plastic strain reaches its maximum value on the compression side and at the onset of fracture. On the basis of the graphs in Figure 10 and Figure 11 an appropriate failure criterion would be the point at which the plastic strain on the compression side stops increasing while the corresponding plastic strain on the tension side starts increasing dramatically. For our model, this was observed at an applied 260 mm horizontal displacement of the loading pin which corresponds to a total bending angle of approximately 20° and a curvature of $9.5 \cdot 10^{-5}$ $[mm^{-1}]$. The initial bending angle and curvature of the model were 12° and $5.6 \cdot 10^{-5}$ $[mm^{-1}]$ respectively. The horizontal axis in Figure 11 shows the x-coordinates of the nodes on the separating line at the unloaded state. It can be observed that in this particular scenario, tensile fracture follows the development of the wrinkle after an additional 250 mm of bending displacement and is characterized by being sudden. The results of this work indicate that in such cases when the angle of the cold bend is aggravated by soil movement, pipeline operators should be cautious of the possibility of tensile fracture failure.

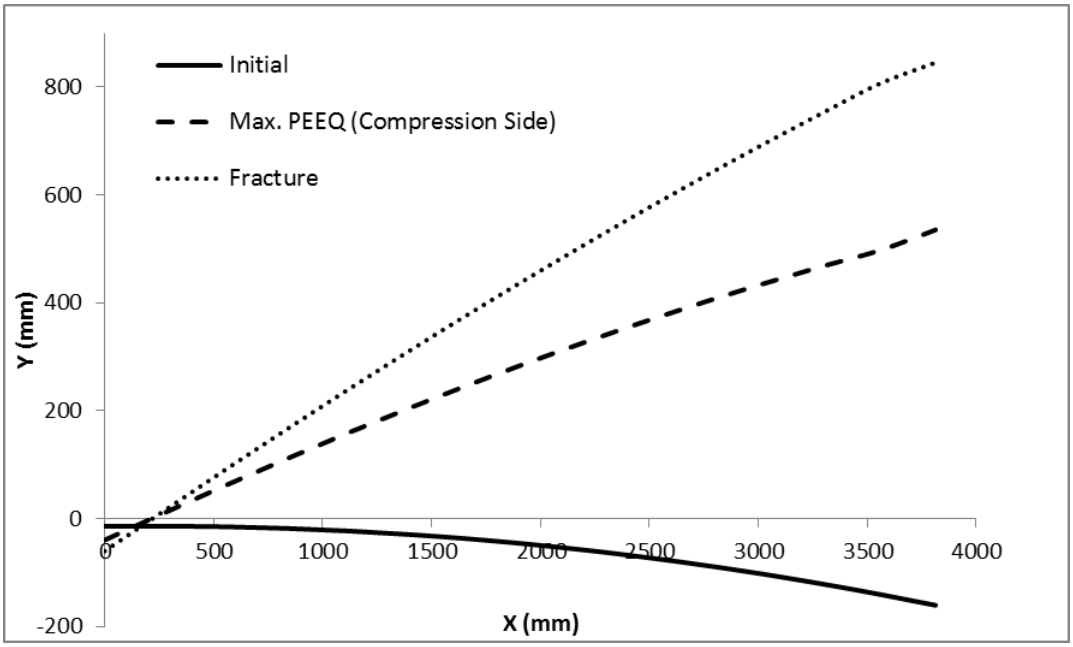

Figure 11: Variation of the displacements in the longitudinal direction

REFERENCES

[1] Sen, M. (2006); "Behaviour of Cold Bend Pipes Under Combined Loads" Ph.D. dissertation, University of Alberta, 2006

[2] Sen, M. , Cheng, J.J.R. , Zhou, J. (2011) ; " Behaviour of Cold Bend Pipes under Bending Loads" DOI: 10.1061/(ASCE)ST.1943-541X.0000219. 2011 American Society of Civil Engineers

[3] Sen, M. , Cheng, J.J.R. , Murray, D. W. (2004) ; "Full-Scale Tests of Cold Bend Pipes" Proceedings of IPC2004, International Pipeline Conference, IPC2004 – 743

[4] Miki, C. , Kobayashi, T. , Oguchi, N. , Uchida, T. , Suganuma, A. , Katoh, A. (2000) ; "Deformation and Fracture Properties of Steel Pipe Bend with Internal Pressure Subjected to In-Plane Bending", Proceedings of the 12th World Conference on Earthquake Engineering